ELSEVIER

Journal of Power Sources 97–98 (2001) 107–113

JOURNAL OF POWER SOURCES

www.elsevier.com/locate/jpowsour

TPD–GC/MS analysis of the solid electrolyte interface (SEI) on a graphite anode in the propylene carbonate/ethylene sulfite electrolyte system for lithium batteries

Hitoshi Ota[a,*], Tomohiro Sato[b], Hitoshi Suzuki[b], Takao Usami[a]

[a]*Tsukuba Laboratory, Center for Analytical Chemistry and Science, Inc. (CACs), 8-3-1 Chu-o, Ami, Inashiki, Ibaraki 300-0332, Japan*
[b]*Tsukuba Research Center, Mitsubishi Chemical Corporation, 8-3-1 Chu-o, Ami, Inashiki, Ibaraki 300-0332, Japan*

Received 6 June 2000; received in revised form 1 February 2001; accepted 4 February 2001

Abstract

The solid electrolyte interface (SEI) formed on a graphite electrode in the electrolyte system consisting of propylene carbonate (PC) and ethylene sulfite (ES) was investigated by temperature programmed desorption or decomposition–gas chromatography/mass spectrometry (TPD–GC/MS), X-ray photoelectron spectroscopy (XPS), scanning electron microscope (SEM), and chemical analysis in order to analyze the detailed structure of the SEI. It was proved that a lithium-oxy-sulfite film (Li_2SO_3 and/or $ROSO_2Li$) was generated by the reductive decomposition of ES in advance of the decomposition of PC and the structure of the SEI structure significantly depends upon current density. In case of the high current density, the inorganic SEI was first formed at high potential and, around the potential where the intercalation of lithium occurs, the organic SEI was formed later. On the other hand, at a low current density, the SEI composed of only an organic component was immediately formed from the starting potential (1.5 V versus Li/Li^+). As a result, it has become clear that the SEI created by the additive at the initial stage of the potential suppressed the reductive decomposition of PC and plays an important role in the effective SEI formation for intercalation.

Keywords: TPD–GC/MS; Solid electrolyte interfaces; Graphite anode; Ethylene sulfite; Additive

1. Introduction

Propylene carbonate (PC) has excellent performance as the main solvent of electrolytes, because the conductivity of PC-based electrolyte at low temperature is higher than that of ethylene carbonate-based electrolytes. However, it is well known that the PC-based electrolyte is easily decomposed electrochemically on graphite and the intercalation efficiency of lithium is very low [1,2]. Recently, the doping of lithium without decomposing the electrolyte has become possible by adding additives to the PC-based solvent [3–9]. Wrodnigg et al. reported that the decomposition of an electrolyte was suppressed by adding ethylene sulfite (ES) [8]. The solid electrolyte interface (SEI) formed on the graphite was identified by some analytical techniques [10–13]. Aubach et al. found by FT-IR that Li_2CO_3 was formed as the passivating film by adding CO_2 gas using FT-IR [4]. Ein-Eli et al. reported that the SEI of Li-oxy-sulfur was generated by adding SO_2 gas [6]. However, in the PC-based electrolyte containing the additives, the structure of the SEI formed on the graphite has not been fully clarified. Therefore, it is very important to clarify the behavior of SEI formation on a graphite and the role of the additives because these SEI possibly change depending upon the charge–discharge conditions such as current density. In this paper, we examined the structure of the SEI formed on a graphite by temperature programmed desorption or decomposition–gas chromatography/mass spectrometry (TPD–GC/MS) in the case that ES was added to the PC solvent. X-ray photoelectron spectroscopy (XPS), scanning electron microscope (SEM) and a chemical analysis method were also used in order to analyze the SEI in detail.

In addition, we report the generation mechanism of the SEI in 1 M $LiPF_6$/PC + ES electrolyte on a graphite anode based on current density.

2. Experimental

Synthetic graphite (KS44) provided by Timcal G&T was used as the carbon electrode and lithium metal foil was used

* Corresponding author. Tel.: +81-298-87-1019; fax: +81-298-88-0337.
E-mail address: 3805359@cc.m-kagaku.co.jp (H. Ota).

0378-7753/01/$ – see front matter
PII: S0378-7753(01)00738-8

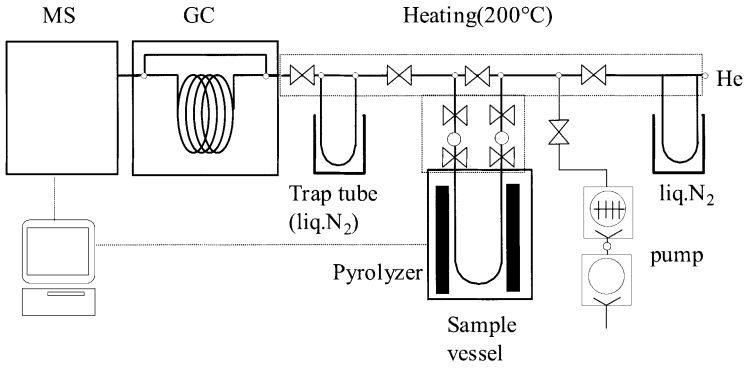

Fig. 1. Schematic diagram of the TPD–GC/MS apparatus.

as the counter electrode. The electrolyte of 10 wt.% ES in PC including 1 M $LiPF_6$ was used. The discharging experiment was carried out using a two-electrode cell. The cell was discharged to 1.5, 0.6 and 0 V versus Li/Li^+ at constant current, 0.008 and 1.6 mA/cm^2.

The organic components of the SEI are generally decomposed below 200°C. The analysis of the SEI structure was carried out by GC/MS (TPD–GC/MS, ANELVA AGS-7000). The schematic diagram of the TPD–GC/MS apparatus is shown in Fig. 1. The graphite anode was heated under helium at the rate of 10°C/min, and the evolved gas up to 200°C was collected in a trap cooled by liquid nitrogen. The collected decomposition gas was introduced into the GC/MS unit by heating the trap. By introducing the gas directly into the MS without using a column, the temperature profile of the decomposition behavior and the quantitative analysis of the organic SEI were carried out (TPD–MS mode). In order to analyze the SEI quantitatively, amount of Li^+, CO_3^{2-}, SO_4^{2-} and F^- ion were determined by using ion chromatography (IC, Dionex IC-4040i). XPS (ULVAC-PHI 5700ci) was used in order to obtain the information on the elementary chemical state of the SEI on the graphite anode. The surface morphology of the film was observed using a SEM (JEOL JSM-6300F). All analysis except for the chemical analysis were done by transporting the samples to the analysis chamber using an inactive transfer vessel.

3. Results and discussion

3.1. Potential curves

The potential curves using 1 M $LiPF_6$/PC electrolyte and 1 M $LiPF_6$/PC + ES 10% electrolyte are shown in Fig. 2. In the electrolyte containing only PC solvent, a constant plateau in the potential curve was observed around 0.9 V due to the successive decomposition of PC. However, the intercalation of lithium can be achieved by adding ES to the electrolyte. At the discharge rate of 1.6 mA/cm^2, the first cycle intercalation efficiency of lithium was 88%. At the low discharge rate of 0.008 mA/cm^2, it was 79%. In case of the low current density, the irreversible capacity increased since the plateau appeared in a higher potential.

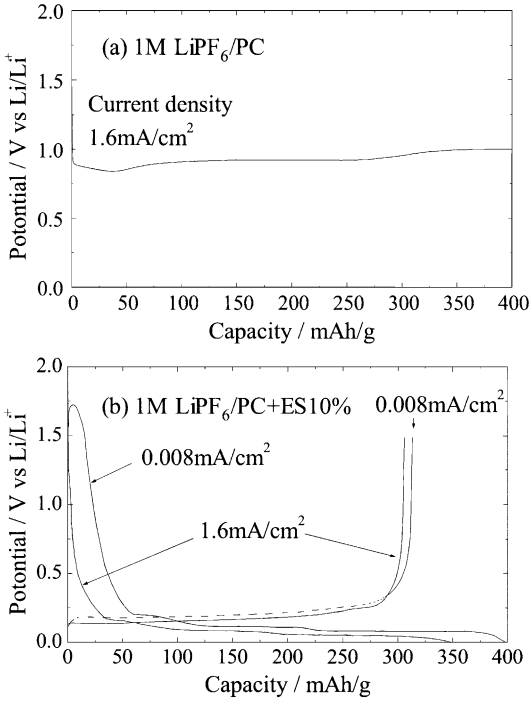

Fig. 2. First discharge–charge curves at various current densities in: (a) 1 M$LiPF_6$/PC; (b) 1 M $LiPF_6$/PC + ES 10% electrolyte.

3.2. TPD–GC/MS analysis of the SEI formed under various conditions

Fig. 3 shows the TPD–GC/MS chromatograms of the SEI formed under various potentials and current densities for the 1 M $LiPF_6$/PC + ES 10% electrolyte system. As for the thermal decomposition of the SEI formed at a low current density, propylene glycol ($CH_3CH(OH)CH_2OH$; PG), H_2O, CO_2 ($m/e = 22$ or 44) and SO_2($m/e = 48$ or 64) were detected at the potential of 1.5V as shown in Fig. 3. These gases were evolved by the thermal decomposition of the SEI, because they were not detected for the sample soaked in the

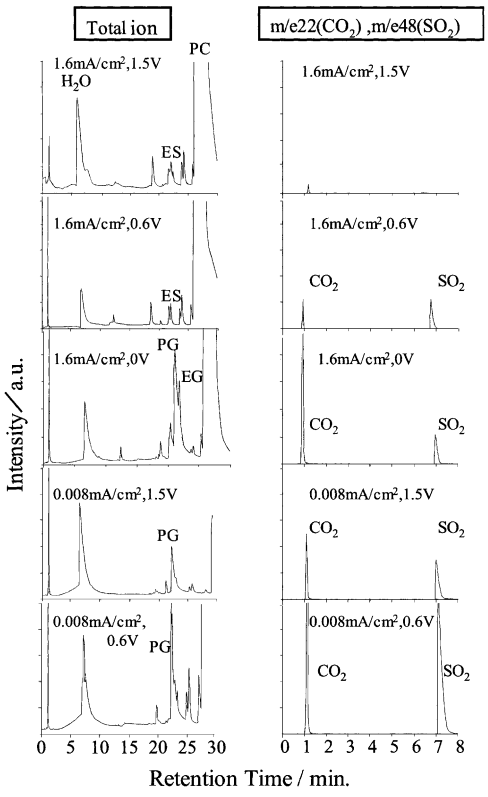

Fig. 3. TPD–GC/MS pattern of SEI at various potential and current density in 1 M $LiPF_6$/PC + ES 10% electrolyte.

electrolyte. In the high current density of 1.6 mA/cm^2, these gas evolution from the SEI was not significantly detected from 1.5 to 0.6 V, and CO_2, SO_2, PG and ethylene glycol (CH_2OHCH_2OH; EG) were main decomposed gas species at 0.6 V or lower. It is expected that these gas species were formed by decomposing lithium alkyl carbonate ($ROCO_2Li$) or lithium alkyl oxy-sulfite ($ROSO_2Li$) according to the reaction scheme (Eqs. 1–3). The one-electron reduction of PC solvent has been proposed by Aurbach et al. [14].

$$2PC + 2Li^+ + 2e^- \rightarrow CH_3CH(OCO_2Li)CH_2OCO_2Li + CH_3CH{=}CH_2 \uparrow \quad (1)$$

$$2ES + 2Li^+ + 2e^- \rightarrow (CH_2OSO_2Li)_2 + CH_2{=}CH_2 \uparrow \quad (2)$$

$$PC + ES + 2Li^+ + 2e^- \rightarrow CH_3CH(OSO_2Li)CH_2OCO_2Li + CH_2{=}CH_2 \uparrow \quad (3)$$

Thermal decomposition:

$$CH_3CH(OSO_2Li)CH_2CO_2Li + 2H_2O \rightarrow CH_3CH(OH)CH_2OH \uparrow + CO_2 \uparrow + SO_2 \uparrow + 2LiOH \downarrow \quad (4)$$

For the solvent system including ES $(CH_2OSO_2Li)_2$ was expected to be created by the one-electron reduction reaction. Fig. 4 shows the TPD–GC/MS chromatogram of the SEI (0 V) in 1 M $LiPF_6$/ES electrolyte system at 1.6 mA/cm^2.

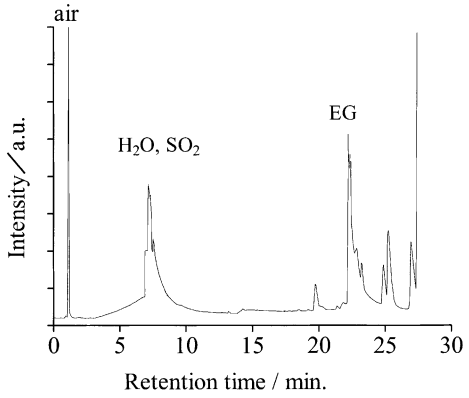

Fig. 4. TPD–GC/MS pattern of SEI in 1 M $LiPF_6$/ES electrolyte.

The detected gas species were mainly SO_2 and EG corresponding to the decomposition of $(CH_2OSO_2Li)_2$. This result suggests that Eq. (2) occurs. In case of the low current density, the thermally decomposed gas from the SEI created around 0.6 V was not EG but PG. This result implies that not only the reductive decomposition of ES but also the decomposition of PC occurs.

3.3. The SEI decomposing behavior as a function of temperature by TPD–MS

The temperature profile of the evolved gas species, CO_2 and SO_2, was monitored by TPD–MS (Fig. 5). It is necessary to choose the mass number so that the fragment of those gas

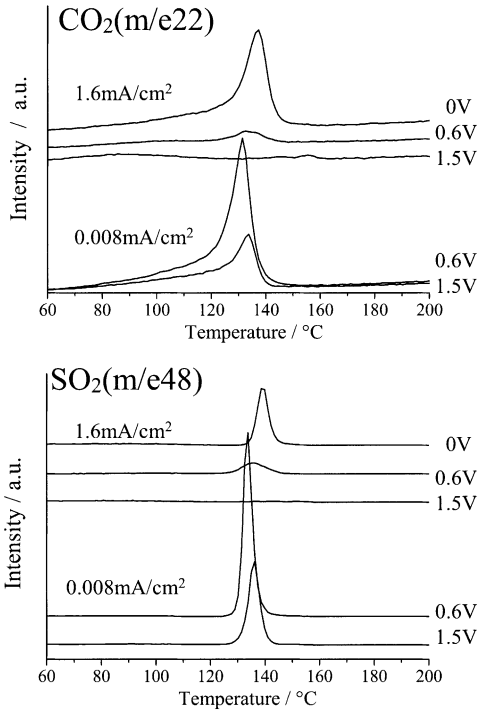

Fig. 5. TPD–MS profile of SEI at various potentials and current densities in 1 M $LiPF_6$/PC + ES 10% electrolyte.

species may not overlap with those from other components in order to obtain the accurate temperature profile. Since the main peak of CO_2 ($m/e = 44$) overlaps with peaks such as the solvent which remains in the SEI, CO_2 is monitored at $m/e = 22$ and the mass number of $m/e = 48$ was chosen for SO_2. It was found that the SEI decomposed around 135°C for both CO_2 and SO_2. For the SEI formed at 1.5 V, corresponding to the above result of TPD–GC/MS, the peaks of CO_2 and SO_2 were not detected at the high current density while those gas species were detected at the low current density. The difference indicates that the irreversible capacity is larger in low current density than high current density.

3.4. Characterization of the structure for the SEI by TPD–GC/MS and chemical analysis

Table 1 shows the quantitative results for the SEI by TPD–MS and chemical analysis. Concerning chemical analysis, in low current density, CO_3^{2-} and SO_4^{2-} ions were mainly detected in the high potential region while, in high current density, only SO_4^{2-} ion was dominantly detected in the high potential region from 1.5 to 0.6 V. As for the CO_3^{2-} and SO_4^{2-} ions, they were originated from the carbonate compound ($ROCO_2Li$, Li_2CO_3) and oxy-sulfite compounds ($ROSO_2Li$, Li_2SO_3), respectively, although the water added for the chemical analysis converted various S species to the SO_4^{2-} ion. In low current density, the amount of SO_4^{2-} by the chemical analysis are in good agreement with the amount of SO_2 by TPD–MS. On the other hand, at the high current density, the amount of SO_4^{2} from the chemical analysis is larger than the amount of SO_2 by TPD–MS. Since the value of the chemical analysis includes the organic and the inorganic SEI and the quantitative results by TPD–MS was obtained only for the organic SEI, it is estimated that at the high current density, fairly amount of the inorganic SEI was generated. About the F^- ion assigned to LiF has been generated at the high potential regardless of current density. The formation of LiF at the high current density is more abundant than that at the low current density. The amount of F^- ion was one-fifth or less than that of the CO_3^{2-}, SO_4^{2-} ion species.

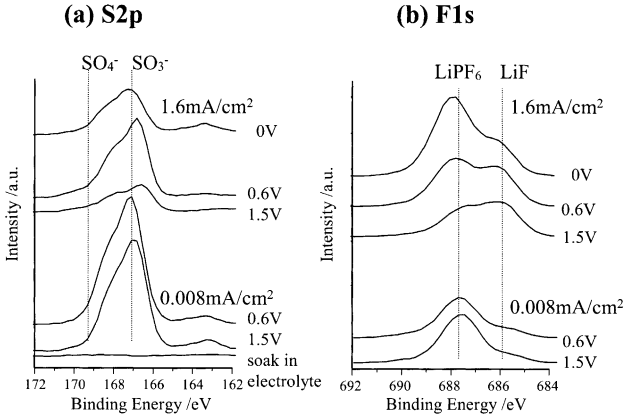

Fig. 6. XPS spectra of S 2p (a) and F 1s (b) of SEI at various potentials and current densities in 1 M $LiPF_6$/PC + ES 10% electrolyte.

3.5. Characterization of the structure for the SEI by XPS and SEM

The chemical state of S was analyzed by XPS. In the S 2p XPS spectra of the SEI, the peak assigned to the SEI appeared at 167.1 eV (Fig. 6a) because the signal was not detected for the sample soaked in the electrolyte. The S 2p peak is composed of S $2p_{3/2}$ and S $2p_{1/2}$, and the half-value width of the signal was 2.2 eV. By considering that the half-value width of a single component was 2.1 eV, the SEI is composed of one component. Based on the chemical shift, the peak at 167.1 eV is assigned to SO_3 species like Li_2SO_3 and $ROSO_2Li$, not to SO_4 species around 169.3 eV. According to the results by TPD–MS, chemical analysis and XPS, it was concluded that ES formed an inorganic SEI (Li_2SO_3) by the two-electron reduction at a high current density at 1.5 V.

$$ES + 2Li^+ + 2e^- \rightarrow Li_2SO_3 \downarrow + CH_2 = CH_2 \uparrow \quad (5)$$

Table 1
Content in the SEI by TPD–MS method and chemical analysis method

Current density	Potential Li/Li$^+$ (V)	Content in the film (mmol/g)					
		By TPD–MS (organic component)			By chemical analysis (total)		
		CO_2	SO_2	CO_3^{2-}	SO_4^{2-}	F^-	Li^+
1.6 mA/cm^2	1.5	0.04	0.03	0.1	0.29	0.07	0.35
	0.6	0.07	0.14	0.09	0.43	0.08	0.62
	0	0.32	0.34	0.94	0.47	0.09	1.68
0.008 mA/cm^2	1.5	0.65	0.22	0.73	0.24	0.03	1.13
	0.6	1.55	0.53	2.13	0.58	0.04	2.88
Composition		$ROCO_2Li$	$ROSO_2Li$	$ROCO_2Li$ Li_2CO_3	ROSOOLi Li_2SO_3	LiF	

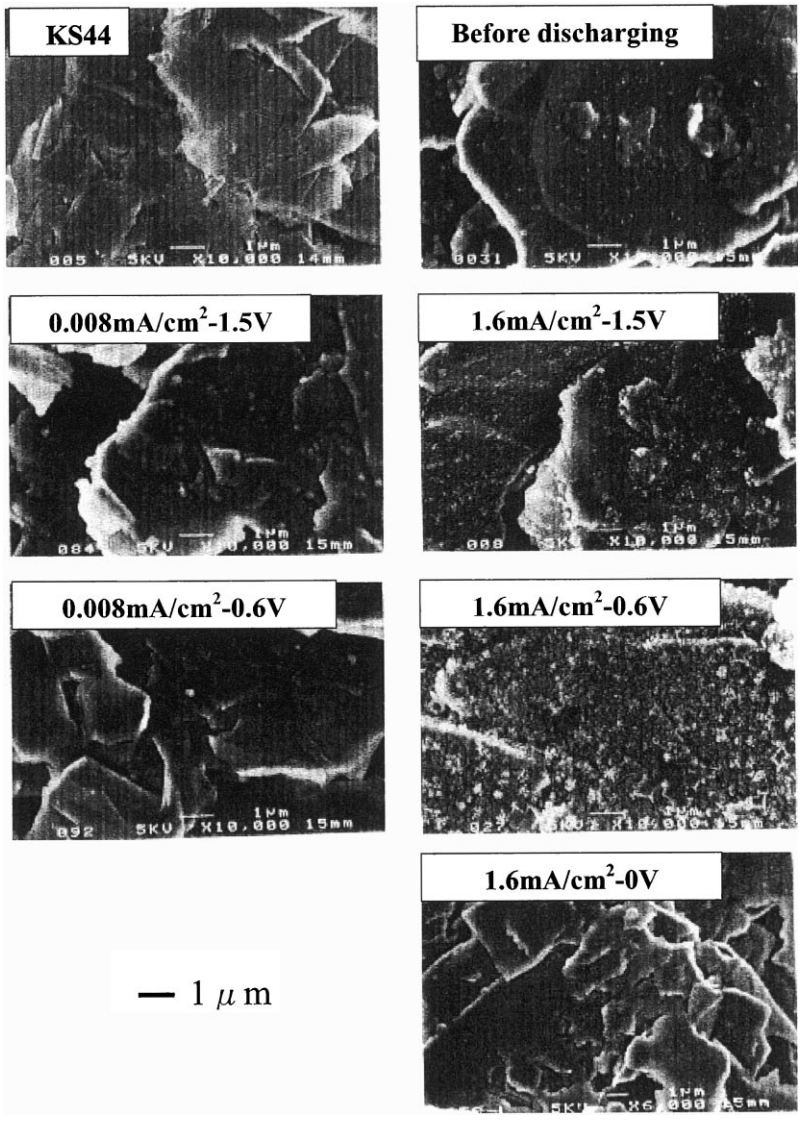

Fig. 7. SEM images of SEI at various potentials and current densities in 1 M $LiPF_6$/PC + ES 10% electrolyte.

Fig. 6b shows the peak of F 1s. The F 1s peak assigned to LiF and $LiPF_6$ were expected to appear around 686 and 687.8 eV, respectively. Therefore, at the low current density, LiF did not exist while LiF was detected at the high current density. Especially, LiF was mainly detected at the high potential. The XPS data correspond to the results by chemical analysis very well.

Fig. 7 shows the SEM images of the SEI at various potentials and in various current densities for the 1 M $LiPF_6$/PC + ES 10% electrolyte system. For the high current density, the SEM images from 1.5 to 0.6 V show the existence of fine particles on the electrode surface while the smooth surface of SEI was observed at 0 V. For the low current density, a smooth film covering the entire graphite surface was observed from 1.5 to 0.6 V. By considering results by other methods, the particulate SEI in high current

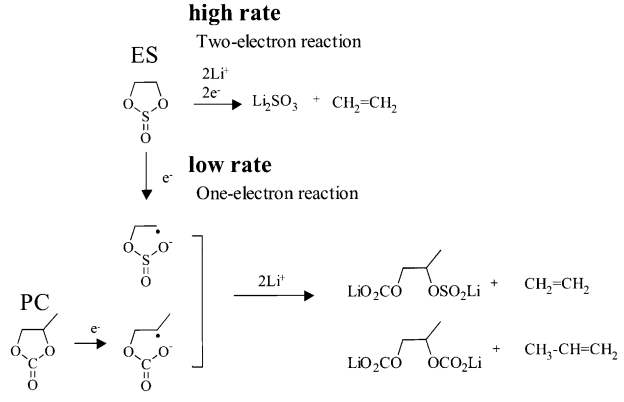

Scheme 1.

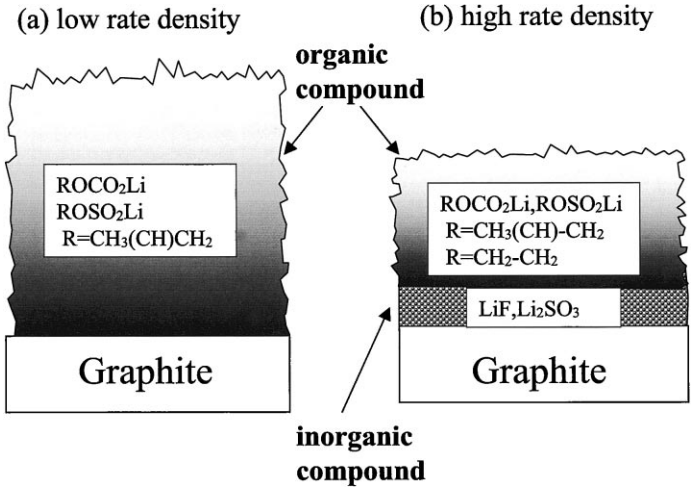

Fig. 8. Schematic illustration of SEI in $LiPF_6$/PC + ES electrolyte.

density seems to be the inorganic SEI and the smooth surface film is possibly assigned to the organic SEI.

3.6. The formation mechanism and structure of the SEI in 1 M $LiPF_6$/PC + ES electrolyte system

The electrochemical reaction in the 1 M $LiPF_6$/PC + ES electrolyte system on the graphite electrode is shown in Scheme 1. Solvated ES receives one-electron, and the ES radical anion is formed. For the high current density, Li_2SO_3 is formed by a two-electron reduction. For the low current density, $CH_3CH(OSO_2Li)CH_2OCO_2Li$ and $CH_3CH(OCO_2Li)CH_2OCO_2Li$ are formed by the electrochemical reaction between the PC radical and ES radical. The difference of the SEI formation behaviors on current density implies that the current density influences the electronic injection rate. The injection of the electron takes rather long time in the low current density and the reaction progresses in the one-electron reaction scheme because the life time of the radical anion/Li^+ can be too short comparing with the time needed for two-electron injection. On the other hand, the injection of two-electron can be easily attained at the high current density. The schematic diagram of the SEI formed on the graphite are shown in Fig. 8. The thick organic films are formed at the low current density. For the high current density, thin inorganic SEI are first formed on the graphite surface at a high potential before intercalation and the organic SEI are formed later on the inorganic films. Since inorganic SEI film formed at the high current density is particulate morphology, the active graphite surface exists. Therefore, it is considered that it reduces solvated Li further and it formed organic SEI by one-electron reduction. Because inorganic SEI film formed at the high current density is not gel-type morphology but particulate morphology, the active graphite surface exists. Therefore, it is considered that the organic films are formed by one-elctron reduction of solvated Li^+ ions further.

4. Conclusions

The formation process of the SEI formed on the graphite anode in a 1 M $LiPF_6$/PC + ES system was analyzed by TPD–GC/MS, chemical analysis, XPS and SEM. From those results, the conclusions described below were derived.

1. The SEI including sulfur constituents was formed in high potential region around 1.5 V versus Li/Li^+ in advance of the reductive decomposition of PC.
2. For the high current density, the inorganic SEI components (Li_2SO_3 and/or LiF) were formed first. The organic SEI($ROCO_2Li$, $ROSO_2Li$ etc.) was formed later around the potential where the intercalation of lithium occurs.
3. For the low current density, the SEI was composed of organic components ($CH_3CH(OSO_2Li)CH_2OCO_2Li$ etc.) from the initial stage.
4. Based on these results, it was confirmed that the SEI structure significantly differed depending upon current density. The decomposition of the additives plays an important role in the effective SEI formation for intercalation.

Acknowledgements

The authors thank Mr. K. Iijima for his helpful assistance with the chemical analysis measurements.

References

[1] A.N. Dey, B.P. Sullivan, J. Electrochem. Soc. 117 (1970) 220.
[2] M. Arakawa, J. Yamaki, J. Electroanal. Chem. 219 (1987) 273.
[3] Z.X. Shu, R.S. McMillan, J.J. Murray, J. Electrochem. Soc. 140 (1993) 922.
[4] D. Aurbach, Y. Ein-Eli, O. Cusid, Y. Carmeli, M. Babai, H. Yamin, J. Electrochem. Soc. 141 (1994) 603.

[5] Z.X. Shu, R.S. McMillan, J.J. Murray, I.J. Davidson, J. Electrochem. Soc. 143 (1996) 2230.
[6] Y. Ein-Eli, S.R. Thomas, V.R. Koch, J. Electrochem. Soc. 142 (1997) 1159.
[7] C. Wang, H. Nakamura, H. Komatsu, M. Yoshio, H. Yoshitake, J. Power Sources 74 (1998) 142.
[8] G.H. Wrodnigg, J.O. Besenhard, M. Winter, J. Electrochem. Soc. 146 (1999) 470.
[9] D.L. Foster, W.K. Behl, J. Wolfenstine, J. Power Sources 85 (2000) 299.
[10] M. Inaba, Z. Siroma, Y. Kawatate, A. Funabiki, Z. Ogumi, J. Power Sources 68 (1997) 221.
[11] K.A. Hirasawa, T. Sato, H. Asahina, S. Yamaguchi, S. Mori, J. Electrochem. Soc. 144 (1997) L81.
[12] A. Naji, J. Ghanbaja, P. Willmann, D. Billaud, J. Power Sources 81/82 (1999) 207.
[13] A.M. Andersson, K. Edström, J.O. Thomas, J. Power Sources 81/82 (1999) 8.
[14] O. Chusid, Y. Ein-Eli, D. Aurbach, M. Babai, Y. Carmeli, J. Power Sources 43/44 (1993) 47.